On the stability of rate-dependent solids with application to the uniaxial plane strain test

Miroslav Nestorović, Yves Leroy, Nicolas Triantafyllidis

On the stability of rate-dependent solids with application to the uniaxial plane strain test

M.D. Nestorovic[a], Y.M. Leroy[b], N. Triantafyllidis[a,*]

[a]Department of Aerospace Engineering, The University of Michigan, Ann Arbor, USA
[b]Laboratoire de Mécanique des Solides, Ecole Polytechnique CNRS UMR 7649, Palaiseau, France

The linear stability criterion, proposed for structural models in an earlier paper, is now extended for a general class of elastic–viscoplastic continua. The time-dependent trajectories, whose stability is under investigation, are functions of two characteristic times: the relaxation time of the viscous solid and the rate of the applied loading, with their ratio denoted by T. It is assumed that the loading conditions of the trajectory are not modified by the perturbation. The criterion predicts that a solid is initially unstable if there exists a unit norm perturbation in the velocity field whose time derivative is positive. This condition is equivalent to finding a positive eigenvalue in the self-adjoint part of the operator relating the initial first and second rate of the displacement perturbations. If the dominant eigenvalue is obtained from the non self-adjoint operator, the change in sign of its real part is a sufficient condition for instability. For solids with an associated flow rule, it is shown that the exclusion of instability in a trajectory, in the limit of vanishing T, coincides with stability of the corresponding rate-independent solid in the sense of Hill. The theory is applied to the analysis of a finitely strained rectangular block under uniaxial tension and compression, for different elastic–viscoplastic solids of the von Mises and Drucker–Prager type.

Keywords: Stability and bifurcation; Viscoplasticity; Uniaxial plane strain compression and tension test

* Corresponding author.

1. Introduction

A linear stability criterion is proposed for elastic–viscoplastic solids, based on the analysis of the initial evolution of small perturbations, and is a generalization of the criterion for the structural models presented by Massin et al. (1999), to be referred hereafter as paper 1. This criterion captures the onset of instability in time-dependent paths (trajectories) of strain-rate sensitive, cohesive and frictional materials which undergo finite straining. Stability at a finite time is not studied thereafter, and the interested reader is referred to paper 1 for a critical review of this question and some illustrative examples.

The motivation for the development of this linear stability criterion is discussed extensively in paper 1 and need not be repeated here, save for the main points. The difficulty in solving the perturbation equations for elastic–viscoplastic solids stems from their non-autonomous nature and spatial discontinuities of their coefficients, due to unloading. Hence, two approaches have emerged: the first extends the work of Hutchinson (1974) on rate-independent solids and consists of following the development of an initial imperfection (e.g. Tvergaard, 1985). Such analyses almost invariably require detailed numerical calculations. The second approach is often analytical and consists of ignoring the time-dependence of the coefficients in the perturbation equations (e.g. Clifton, 1978; Leroy, 1991 and Molinari, 1997). The validity of this so-called frozen coefficients method requires that the perturbation rate is much larger in magnitude than the rate of the fundamental solution. This requirement is not met at the stability transition, as pointed out by Anand et al. (1987).

The first step towards the development of a general linear stability criterion for elastic–viscoplastic solids, presented in paper 1, uses two versions of Shanley's column (Shanley, 1947). There, the stability transition was defined by the change in sign of the second time-derivative of the column's angular position evaluated at the onset of perturbation. Two characteristic times have been identified: the first is the relaxation time of the viscous supports and the second is the rate of the applied loading. The ratio of these two times defines the dimensionless number T, which vanishes if the structure is in equilibrium. It was found that the stability transition for principal equilibria (i.e., for the straight configuration of the columns) occurs at the reduced modulus load, which is the classical critical load for rate-independent columns, if the stability criterion is based on the maximum dissipation (Nguyen and Radenkovic, 1975). If the proposed criterion is used to investigate the principal trajectories for arbitrary values of T, and for adequately small values of the initial perturbation to avoid initial unloading, the stability transition occurs at a critical load named the rate-dependent tangent modulus load. This critical load is a decreasing function of T, converging to the classical tangent modulus load in the limit of inviscid plastic flow, i.e., in the limit of vanishing T.

The objective of this paper is to generalize the above described linear stability criterion for the case of strain-rate dependent, frictional, cohesive continua under finite strains, assuming that the perturbation does not modify the loading

conditions of the trajectory under investigation. The role of the column rotation rate from paper 1 is now played by the norm of admissible perturbations in the velocity field. The transition to instability is marked by the change in sign from negative to positive of the maximum initial time-derivative of the norm of all admissible velocity perturbations. The possibility of an elastic unloading at the onset of perturbation, which was also studied in paper 1, is postponed for the sequel of this work.

The contents of this paper are as follows: Section 2 pertains to the presentation of the linear stability criterion. First, the governing equations for a general class of rate-dependent solids are recorded, followed by the derivation of the conditions prevailing at the end of the perturbation sequence, called the onset. Subsequently, the equations governing the time evolution of the perturbation are obtained from the first and second time-derivatives of the principle of virtual work. The linear stability criterion requires the search for the maximum derivative with respect to time of the perturbation velocity norm, a positive sign signaling the initial instability. This task is identical to finding a maximum eigenvalue of the self-adjoint part of the operator relating the initial first and second rate of the displacement perturbations. A sufficient condition for linear instability is given by a positive real part of the maximum eigenvalue of the non self-adjoint operator. Section 3 pertains to the limit of inviscid plastic flow, attained for vanishing T. It is found, for the case of a rate-independent solid with an associated flow rule, that the exclusion of instability in a trajectory implies the positive definiteness of the quadratic stability functional for the elastic–plastic comparison solid. Hence, the linear stability criterion coincides with the result given by Hill (1958) for the same class of rate-independent solids. For simplicity, all the calculations in Sections 2 and 3 are presented in the context of small strain, moderate rotations. The generalization to finite strains is outlined in Appendix A.

In Section 4, the criterion is applied to the analysis of the finite plane strain tension and compression of a rectangular block composed of a rate-dependent version of either a von Mises solid or a Drucker–Prager frictional, cohesive material. Two different models of rate-dependence are considered, a linear overstress and a power-law type model. The details of the stability analysis are found in Appendix B. The results are presented in terms of critical strains and stresses, i.e., quantities evaluated at the stability transition, as functions of T. The influence of geometry, constitutive law and dimensionless number T on the stability results is discussed at the end of Section 4.

2. Linear stability analysis

The objective of this section is the concise presentation of the proposed linear stability analysis for strain-rate dependent solids. In the interest of algebraic simplicity, the theory is presented without loss of generality, in the context of small strain, moderate rotations. In this form, the stability criterion is applicable

to structural problems such as beams, plates and shells. The generalization to finite strains is outlined in Appendix A.

This section is divided into three parts. The governing equations are recorded first, followed by the perturbation analysis. The formulation of the eigenvalue problem, the key element of the linear stability analysis, is discussed in the third part.

2.1. Governing equations

Consider a solid occupying the volume V bounded by the surface ∂V. The inertia effects are disregarded and in the absence of body forces, for equilibrium to be satisfied, the principle of virtual work dictates:

$$\int_V \boldsymbol{\sigma}:\delta\boldsymbol{\epsilon}\,\mathrm{d}V = \int_{\partial V} \mathbf{T}\cdot\delta\mathbf{u}\,\mathrm{d}S, \tag{1}$$

where $\boldsymbol{\sigma}$ is the Cauchy stress tensor, $\boldsymbol{\epsilon}$ is its work conjugate strain measure (a function of the displacement $\mathbf{u}$) and $\mathbf{T}$ is the traction prescribed on a subset of the domain's boundary ∂V. A dot and a colon denote the classical inner products of vectors and second-order tensors, respectively, ($\mathbf{a}\cdot\mathbf{b} = a_i b_i$, $\mathbf{A}:\mathbf{B} = A_{ij}B_{ij}$ for any vectors $\mathbf{a}$ and $\mathbf{b}$, and any second-order tensors $\mathbf{A}$ and $\mathbf{B}$ in a Cartesian coordinate system). The following non-linear kinematics relation is adopted:

$$\boldsymbol{\epsilon} = \frac{1}{2}(\mathbf{u}\nabla + \nabla\mathbf{u} + \nabla\mathbf{u}\cdot\mathbf{u}\nabla), \tag{2}$$

where the symbol ∇ is the gradient operator[1]. The strain tensor $\boldsymbol{\epsilon}$ is decomposed into an elastic (reversible) and a plastic (irreversible) part, the latter denoted by $\boldsymbol{\epsilon}^{\mathrm{p}}$. The stress is related to the elastic strain by:

$$\boldsymbol{\sigma} = \mathbf{L}^{\mathrm{e}}:(\boldsymbol{\epsilon} - \boldsymbol{\epsilon}^{\mathrm{p}}), \tag{3}$$

where $\mathbf{L}^{\mathrm{e}}$ is the fourth-order linear elasticity tensor. A constitutive model with a single internal variable (γ, the equivalent plastic strain) is adopted for simplicity, according to which the orientation of the plastic strain rate in stress space is along the normal to the flow potential $\psi(\boldsymbol{\sigma})$,

$$\frac{\mathrm{d}\boldsymbol{\epsilon}^{\mathrm{p}}}{\mathrm{d}t} = \frac{\mathrm{d}\gamma}{\mathrm{d}t}\frac{\partial\psi}{\partial\boldsymbol{\sigma}}. \tag{4}$$

The accumulated plastic strain rate is written as

$$\frac{\mathrm{d}\gamma}{\mathrm{d}t} = \frac{1}{t_{\mathrm{R}}}\mathscr{H}\big[F\big(\phi(\boldsymbol{\sigma}), g(\gamma), t_{\mathrm{R}}\big)\big], \tag{5}$$

[1] In a Cartesian basis $\{\mathbf{e}_i\}$, ∇ is equal to $\mathbf{e}_i\partial/\partial x_i$ such that $\nabla\mathbf{a}$ and $\mathbf{a}\nabla$ are the tensors: $a_{i,j}\mathbf{e}_j\otimes\mathbf{e}_i$ and $a_{i,j}\mathbf{e}_i\otimes\mathbf{e}_j$, respectively, for any vector $\mathbf{a}$. A comma in the subscript denotes partial differentiation.

where the function F has for arguments: $\phi(\boldsymbol{\sigma})$, $g(\gamma)$ and t_R which are an equivalent stress, a hardening function of the accumulated plastic strain γ and the relaxation time of the material, respectively. Note that the Heaviside function $\mathscr{H}$ in Eq. (5) is equal to zero if the function F is negative, signaling an elastic response of the material. The time-dependency of the material response has resulted in the introduction of a relaxation time t_R in Eq. (5). The details of its definition depend on the choice of a viscosity function, but all definitions should share the common feature that t_R tends to zero for vanishing viscosity. In that instance, F tends also to zero, providing the yield criterion of the corresponding rate-independent material, i.e., the equivalent stress $\phi(\boldsymbol{\sigma})$ is then equal to $g(\gamma)$.

By controlling tractions or displacements on the boundary, the solid described above sustains a time-dependent deformation process which is referred to as the fundamental trajectory and is denoted by an "o" in subscript. The fundamental trajectory, whose stability is the goal of this investigation, depends on the rate at which the loading is applied, thus introducing a characteristic time t_L. The ratio of the two characteristic time scales is the dimensionless number T

$$T \equiv \frac{t_R}{t_L}, \tag{6}$$

which has a zero value either for a zero viscosity or for a loading independent of time. In both cases, the zero value of T signals a fundamental equilibrium solution. Henceforth, all equations are written in terms of the dimensionless time τ, defined by $\tau \equiv t/t_L$, and all derivatives with respect to τ are represented by a superposed dot.

2.2. Perturbation analysis

The objective of this subsection is to determine the initial evolution of the perturbation. First, the structure of the perturbation sequence is explained, resulting in the initial conditions for the perturbation problem. Second, the boundary value problem for the initial evolution of the perturbation is derived in terms of the initial velocity of perturbation and its rate.

The perturbation of the fundamental solution starts at time $\tau^* - \Delta\tau$ and lasts for a duration $\Delta\tau$, and is realized by a modification of the applied boundary tractions. These boundary tractions remain constant in time beyond τ^*, which is referred to as the "onset" in the rest of the paper. The physical time interval of the perturbation is assumed to be small compared to the two time scales of the problem, i.e., $\Delta\tau \ll 1$ and $\Delta\tau \ll T$. The symbol Δ is used to denote the difference between quantities estimated along the fundamental trajectory and the perturbed one, namely: $\Delta A(\tau) \equiv A(\tau) - A_o(\tau)$, in which A is a generic name for any field variable.

The initial conditions for the evolution problem are now derived assuming continuity in time of all the field variables during the perturbation sequence. The perturbation in plastic strain and in the internal variable are found to be at

time τ^*

$$\Delta\boldsymbol{\epsilon}^{\mathrm{p}}(\tau^*) = \int_{\tau^*-\Delta\tau}^{\tau^*} \Delta\dot{\boldsymbol{\epsilon}}^{\mathrm{p}}(\tau)\,\mathrm{d}\tau = \frac{\Delta\tau}{T}\left(F_{,\phi}\frac{\partial\psi}{\partial\boldsymbol{\sigma}}\frac{\partial\phi}{\partial\boldsymbol{\sigma}} + F\frac{\partial^2\psi}{\partial\boldsymbol{\sigma}\partial\boldsymbol{\sigma}}\right):\Delta\boldsymbol{\sigma} + \mathcal{O}\left[\left(\frac{\Delta\tau}{T}\right)^2\right],$$

$$\Delta\gamma(\tau^*) = \int_{\tau^*-\Delta\tau}^{\tau^*} \Delta\dot{\gamma}(\tau)\,\mathrm{d}\tau = \frac{\Delta\tau}{T}F_{,\phi}\frac{\partial\phi}{\partial\boldsymbol{\sigma}}:\Delta\boldsymbol{\sigma} + \mathcal{O}\left[\left(\frac{\Delta\tau}{T}\right)^2\right]. \tag{7}$$

The above results are obtained by applying the mean value theorem to the integrals and by subsequently replacing the rates of perturbation $\Delta\dot{\gamma}$ and $\Delta\dot{\boldsymbol{\epsilon}}^{\mathrm{p}}$ by their asymptotic expansions, in terms of the small parameter $\Delta\tau/T$, which are obtained by linearizing the constitutive relations (4) and (5). The stress perturbation is then found by inserting these results into the linearized form of Eq. (3),

$$\Delta\boldsymbol{\sigma}(\tau^*) = \boldsymbol{L}^{\mathrm{e}}:\Delta\boldsymbol{\epsilon} + \mathcal{O}\left(\frac{\Delta\tau}{T}\right). \tag{8}$$

These calculations lead to the conclusion that the perturbation in stress at time τ^* can be approximated, to the first order in $\Delta\tau/T$, by the elastic response of the solid. The perturbations in plastic strain (7) are thus disregarded compared to the strain perturbations, since they are of higher order in the small parameter $\Delta\tau/T$. It should be stressed that Eq. (8) does not imply that the system has unloaded elastically during the perturbation. On the contrary, the perturbation is assumed to preserve the loading condition satisfied along the fundamental trajectory. Note that the details of the perturbation sequence are nevertheless unimportant for determining the conditions at the onset.

The second objective of this subsection is to determine the relations between the perturbation in displacement $\Delta\mathbf{u}$ and its rates $\Delta\dot{\mathbf{u}}$ and $\Delta\ddot{\mathbf{u}}$. These relations are obtained from the linearized version of the principle of virtual work and its first and second derivatives with respect to time. All equations displayed subsequently are evaluated at τ^*, the onset of perturbation, unless otherwise stated.

The linearized version of the principle of virtual work (1) together with the initial conditions (7) and (8) gives

$$\int_V \delta\mathbf{u}\nabla:\mathbf{L}:\Delta\mathbf{u}\nabla\,\mathrm{d}V = \int_{\partial V}\Delta\mathbf{T}\cdot\delta\mathbf{u}\,\mathrm{d}S,$$
$$\text{where } \mathbf{L} \equiv \mathbf{L}^{\mathrm{e}} + \mathbf{S} \text{ and } S_{ijkl} \equiv \sigma_{oji}\delta_{ik}. \tag{9}$$

To obtain these results, an updated Lagrangian description of motion has been adopted by introducing the simplifying assumption that the displacement along the fundamental trajectory $\mathbf{u}_o$, and thus its gradient $\nabla\mathbf{u}_o$, have been set to zero at time τ^*.

A similar expression to Eq. (9) is now derived to relate the perturbations in displacement and velocity at the onset. For that purpose, the rate form of the principle of virtual work, obtained from Eq. (1) by differentiation with respect to the dimensionless time τ and linearization, yields:

$$\int_V \Delta\dot{\boldsymbol{\sigma}}:\delta\boldsymbol{\epsilon} + \dot{\boldsymbol{\sigma}}_o:\Delta\delta\boldsymbol{\epsilon} + \Delta\boldsymbol{\sigma}:\delta\dot{\boldsymbol{\epsilon}} + \boldsymbol{\sigma}_o:\Delta\delta\dot{\boldsymbol{\epsilon}}\,\mathrm{d}V = 0. \tag{10}$$

Note that the rate of traction perturbation does not appear on the right-hand side of Eq. (10) since that quantity is assumed to be constant in time, once the perturbation sequence has ended.

The following expression is found for the perturbation in plastic strain rate:

$$\Delta\dot{\boldsymbol{\epsilon}}^{\mathrm{p}} = \frac{1}{T}\mathbf{M}:\Delta\boldsymbol{\sigma}, \quad \text{where } \mathbf{M} \equiv F_{,\phi}\frac{\partial\psi}{\partial\boldsymbol{\sigma}}\frac{\partial\phi}{\partial\boldsymbol{\sigma}} + \dot{\gamma}_o T\frac{\partial^2\psi}{\partial\boldsymbol{\sigma}\partial\boldsymbol{\sigma}}, \tag{11}$$

and is obtained by linearization of the constitutive equation (4) and perturbation of the internal variable in $(7)_2$. The fourth-order tensor $\mathbf{M}$ has the major symmetry if associated flow rules are considered (i.e., if $\phi = \psi$). Note that $\mathbf{M}$ is invertible if the second term on the right-hand side of $(11)_2$ differs from zero, a condition always respected along the fundamental trajectory for non-zero values of T.

The result in Eq. (11) permits us to rewrite the linearized rate of the principle of virtual work (10) as

$$\int_V \delta\mathbf{u}\nabla:(\mathbf{L}:\Delta\dot{\mathbf{u}}\nabla + \mathbf{A}:\nabla\Delta\mathbf{u})\,\mathrm{d}V = 0, \tag{12}$$

where the fourth-order tensor $\mathbf{A}$ is defined by:

$$\mathbf{A} \equiv -\mathbf{L}^{\mathrm{e}}:\frac{\mathbf{M}}{T}:\mathbf{L}^{\mathrm{e}} + \dot{\mathbf{R}}_o + \mathbf{L}^{\mathrm{e}}\cdot\nabla\dot{\mathbf{u}}_o + \dot{\mathbf{u}}_o\nabla\cdot\mathbf{L}^{\mathrm{e}}, \tag{13}$$

with $R_{ijkl} = S_{ijlk}$. Note in Eq. (13) that even though the values of $\mathbf{u}_o$ and $\mathbf{u}_o\nabla$ along the fundamental trajectory are set to zero at the onset, their rates cannot be disregarded in the updated Lagrangian formulation of the problem.

As for Shanley's column analysis in paper 1, the operator $\mathbf{L}^{\mathrm{e}}$ characterizes the instantaneous response of the solid, and hence Eq. (12) does not provide any information of interest until the elastic Euler load is approached. For this reason, it is necessary to turn our attention to the second rate of the principle of virtual work to obtain a relation between the perturbation in velocity $\Delta\dot{\mathbf{u}}$ and its rate of change $\Delta\ddot{\mathbf{u}}$. The first step is the linearization of the second derivative with respect to time of the equilibrium equation (1),

$$\int_V \Delta\ddot{\boldsymbol{\sigma}}:\delta\boldsymbol{\epsilon} + \ddot{\boldsymbol{\sigma}}_o:\Delta\delta\boldsymbol{\epsilon} + 2(\Delta\dot{\boldsymbol{\sigma}}:\delta\dot{\boldsymbol{\epsilon}} + \dot{\boldsymbol{\sigma}}_o:\Delta\delta\dot{\boldsymbol{\epsilon}}) + \Delta\boldsymbol{\sigma}:\delta\ddot{\boldsymbol{\epsilon}} + \boldsymbol{\sigma}_o:\Delta\delta\ddot{\boldsymbol{\epsilon}}\,\mathrm{d}V = 0. \tag{14}$$

The procedure to follow is similar to the one considered to obtain Eq. (12), but

the details of the calculation are rather cumbersome. A single intermediate result on the perturbation of the second rate of plastic strain, counterpart of Eq. (11), is recorded

$$\begin{aligned}
&\Delta\ddot{\boldsymbol{\epsilon}}^{\mathrm{p}} = \frac{1}{T}(\mathbf{M}{:}\Delta\ddot{\boldsymbol{\sigma}} + \mathbf{N}{:}\Delta\boldsymbol{\sigma}),\\
&\text{where } \mathbf{N} \equiv F_{,\phi\phi}\frac{\partial\phi}{\partial\boldsymbol{\sigma}}{:}\dot{\boldsymbol{\sigma}}_o\frac{\partial\psi}{\partial\boldsymbol{\sigma}}\frac{\partial\phi}{\partial\boldsymbol{\sigma}} + \dot{\gamma}_o g_{,\gamma}\left(F_{,g}\frac{\partial^2\psi}{\partial\boldsymbol{\sigma}\partial\boldsymbol{\sigma}} + F_{,g\phi}\frac{\partial\psi}{\partial\boldsymbol{\sigma}}\frac{\partial\phi}{\partial\boldsymbol{\sigma}}\right)\\
&\qquad + \dot{\gamma}_o T\frac{\partial^3\psi}{\partial\boldsymbol{\sigma}\partial\boldsymbol{\sigma}\partial\boldsymbol{\sigma}}{:}\dot{\boldsymbol{\sigma}}_o + F_{,\phi}\left(\frac{\partial\phi}{\partial\boldsymbol{\sigma}}{:}\dot{\boldsymbol{\sigma}}_o\frac{\partial^2\psi}{\partial\boldsymbol{\sigma}\partial\boldsymbol{\sigma}} + \frac{\partial\psi}{\partial\boldsymbol{\sigma}}\frac{\partial^2\phi}{\partial\boldsymbol{\sigma}\partial\boldsymbol{\sigma}}{:}\dot{\boldsymbol{\sigma}}_o\right.\\
&\qquad \left. + \frac{\partial^2\psi}{\partial\boldsymbol{\sigma}\partial\boldsymbol{\sigma}}{:}\dot{\boldsymbol{\sigma}}_o\frac{\partial\phi}{\partial\boldsymbol{\sigma}} + \frac{1}{T}F_{,g}g_{,\gamma}\frac{\partial\psi}{\partial\boldsymbol{\sigma}}\frac{\partial\phi}{\partial\boldsymbol{\sigma}}\right).
\end{aligned} \tag{15}$$

With the help of Eq. (15) we obtain the final result relating the zeroth, first and second time-derivatives of the perturbation, i.e.,

$$\int_V \delta\mathbf{u}\nabla{:}(\mathbf{L}{:}\Delta\ddot{\mathbf{u}}\nabla + \mathbf{B}{:}\nabla\Delta\dot{\mathbf{u}} + \mathbf{C}{:}\nabla\Delta\mathbf{u})\,\mathrm{d}V = 0, \tag{16}$$

where the fourth-order tensors $\mathbf{B}$ and $\mathbf{C}$ are found to be:

$$\begin{aligned}
&\mathbf{B} \equiv -\mathbf{L}^{\mathrm{e}}{:}\frac{\mathbf{M}}{T}{:}\mathbf{L}^{\mathrm{e}} + 2\big(\dot{\mathbf{R}}_o + \mathbf{L}^{\mathrm{e}}\cdot\nabla\dot{\mathbf{u}}_o + \dot{\mathbf{u}}_o\nabla\cdot\mathbf{L}^{\mathrm{e}}\big),\\
&\mathbf{C} \equiv \mathbf{L}^{\mathrm{e}}{:}\left(\frac{\mathbf{M}}{T}{:}\mathbf{L}^{\mathrm{e}}{:}\frac{\mathbf{M}}{T} - \frac{\mathbf{N}}{T}\right){:}\mathbf{L}^{\mathrm{e}} + \ddot{\mathbf{R}}_o + \ddot{\mathbf{u}}_o\nabla\cdot\mathbf{L}^{\mathrm{e}} + \mathbf{L}^{\mathrm{e}}\cdot\nabla\ddot{\mathbf{u}}_o\\
&\qquad + 2\dot{\mathbf{u}}_o\nabla\cdot\mathbf{L}^{\mathrm{e}}\cdot\nabla\dot{\mathbf{u}}_o - \mathbf{L}^{\mathrm{e}}{:}\frac{\mathbf{M}}{T}{:}\mathbf{L}^{\mathrm{e}}\cdot\nabla\dot{\mathbf{u}}_o - 2\dot{\mathbf{u}}_o\nabla\cdot\mathbf{L}^{\mathrm{e}}{:}\frac{\mathbf{M}}{T}{:}\mathbf{L}^{\mathrm{e}}.
\end{aligned} \tag{17}$$

With this last result, the stage is ready for studying the initial evolution in time of the perturbation added at τ^* to the system with a known time dependent trajectory.

2.3. Stability criterion

The Eqs. (9), (12) and (16) govern the linearized initial perturbation of a given trajectory and can be rewritten as:

$$\begin{aligned}
&\mathscr{E}[\Delta\mathbf{u}] = \mathscr{T}[\Delta\mathbf{T}],\\
&\mathscr{E}[\Delta\dot{\mathbf{u}}] + \mathscr{A}[\Delta\mathbf{u}] = 0,\\
&\mathscr{E}[\Delta\ddot{\mathbf{u}}] + \mathscr{B}[\Delta\dot{\mathbf{u}}] + \mathscr{C}[\Delta\mathbf{u}] = 0,
\end{aligned} \tag{18}$$

in terms of the linear integro-differential operators, whose definitions are clear from the structure of the corresponding equations. If the operator $\mathscr{A}$ is invertible, a condition guaranteed by the properties of $\mathbf{M}$ discussed after Eq. (11), we find a linear operator $\mathscr{L}$

$$\Delta\ddot{\mathbf{u}} = \mathscr{L}[\Delta\dot{\mathbf{u}}], \tag{19}$$

by combining the last two equations in (18). The only exception foreseen for the existence of this operator is if the operator $\mathscr{E}$, associated with the elastic response of the system, is not invertible. However, no such case is expected here since the instability occurs at loads which are a fraction of the structure's Euler load. Note also that for $T \neq 0$, the operator $\mathscr{L}$ is not in general self-adjoint, even for associated plasticity models, as revealed by inspection of Eqs. (13) and (17).

The proposed linear stability criterion is defined as follows: a trajectory is said to be stable at τ^* if the maximum of the time derivative of the L_2 norm of all admissible perturbations in the velocity field is found to be negative, i.e.,

$$\max\left\{\left[\frac{\mathrm{d}}{\mathrm{d}\tau}\left(\|\Delta\dot{\mathbf{u}}\|^2\right)\right]_{\tau=\tau^*}\right\} < 0 \quad \text{with } (\|\Delta\dot{\mathbf{u}}\|)_{\tau=\tau^*} = 1, \tag{20}$$

which, in view of Eq. (19), is equivalent to:

$$\Lambda^{\mathrm{S}} \equiv \max\left\{\langle\Delta\dot{\mathbf{u}}, \mathscr{L}^{\mathrm{S}}[\Delta\dot{\mathbf{u}}]\rangle_{\tau=\tau^*}\right\} < 0 \quad \text{with } (\|\Delta\dot{\mathbf{u}}\|)_{\tau=\tau^*} = 1, \tag{21}$$

where $\mathscr{L}^{\mathrm{S}}$ denotes the self-adjoint part of the stability operator $\mathscr{L}$. The search for the maximum in Eq. (21) requires finding the dominant eigenvalue Λ^{S}, the largest of all eigenvalues, of $\mathscr{L}^{\mathrm{S}}$.

Analytical expression for the operator $\mathscr{L}^{\mathrm{S}}$ is not easily obtained. Instead, it is more convenient to search for the dominant eigenvalue Λ of the operator $\mathscr{L}$ in Eq. (19), defined as the eigenvalue with the largest real part of the following system:

$$\begin{aligned} &\mathscr{E}[\Delta\dot{\mathbf{u}}] + \mathscr{A}[\Delta\mathbf{u}] = 0, \\ &\Lambda\mathscr{E}[\Delta\dot{\mathbf{u}}] + \mathscr{B}[\Delta\dot{\mathbf{u}}] + \mathscr{C}[\Delta\mathbf{u}] = 0. \end{aligned} \tag{22}$$

Since $\langle\Delta\dot{\mathbf{u}}, \mathscr{L}^{\mathrm{S}}[\Delta\dot{\mathbf{u}}]\rangle = \langle\Delta\dot{\mathbf{u}}, \mathscr{L}[\Delta\dot{\mathbf{u}}]\rangle$, it follows that $\Lambda^{\mathrm{S}} \geq \Lambda$ (the equality holding for symmetric $\mathscr{L}$) and the existence of Λ with a positive real part implies the existence of a positive eigenvalue for $\mathscr{L}^{\mathrm{S}}$, thus proving the linear instability of the system studied. Consequently, direct study of Eq. (22) provides a sufficient condition for instability.

3. Limit of inviscid plastic flow

In this section of interest are the predictions of the proposed linear stability criterion in the limit of inviscid plastic flow ($t_R \to 0$). This limit is equivalent to an infinitely long characteristic loading time ($t_L \to \infty$). To this end, the corresponding rate-independent constitutive law need be recorded, for the case of plastic loading. For $t_R \to 0$, the function F in Eq. (5) must equal zero for the equivalent plastic strain to remain bounded. This condition, which must hold during the loading process, provides the consistency requirement $\dot{F} = 0$, from which the equivalent plastic strain rate is related to the stress rate, i.e.,

$$\dot{\gamma} = -\frac{F_{,\phi}}{F_{,g} g_{,\gamma}} \frac{\partial \phi}{\partial \boldsymbol{\sigma}} : \dot{\boldsymbol{\sigma}}. \tag{23}$$

Combining this result with Eq. (4) and the rate form of Eq. (3) results in the incremental constitutive equation for the corresponding inviscid solid

$$\begin{aligned} &\dot{\boldsymbol{\sigma}} = \left(\mathbf{L}^{e} - \mathbf{Q} H^{-1} \mathbf{P}\right) : \dot{\boldsymbol{\epsilon}}, \\ &\text{where } \mathbf{Q} \equiv \mathbf{L}^{e} : \frac{\partial \psi}{\partial \boldsymbol{\sigma}}, \ \mathbf{P} \equiv \frac{\partial \phi}{\partial \boldsymbol{\sigma}} : \mathbf{L}^{e} \text{ and } H \equiv \frac{\partial \phi}{\partial \boldsymbol{\sigma}} : \mathbf{L}^{e} : \frac{\partial \psi}{\partial \boldsymbol{\sigma}} - \frac{F_{,g}}{F_{,\phi}} g_{,\gamma}. \end{aligned} \tag{24}$$

According to Hill (1958), an equilibrium path is stable if the quadratic functional, based on the elastoplastic incremental moduli of $(24)_1$, is positive definite,

$$\int_V \delta \mathbf{u} \nabla : \left(\mathbf{L} - \mathbf{Q} H^{-1} \mathbf{P}\right) : \delta \mathbf{u} \nabla \, \mathrm{d}V > 0, \tag{25}$$

for all admissible $\delta \mathbf{u}$ and for an associated flow rule ($\phi = \psi$). If the minimum eigenvalue of the functional in Eq. (25) vanishes, a bifurcation away from the principal equilibrium solution is possible. In the case of frictional, cohesive media ($\phi \neq \psi$), a zero minimum eigenvalue also corresponds to a bifurcation. For a class of cohesive, frictional solids investigated by Triantafyllidis and Leroy (1994), it was found that in spite of the non-symmetry of the incremental moduli, the spectrum of the non self-adjoint operator corresponding to Eq. (25) is always real. It is assumed that this condition holds true here. Hence, a change in sign of the dominant eigenvalue of Eq. (25) signals instability.

The remainder of this section demonstrates that in the limit $T \to 0$ the system in Eq. (22), for $\Lambda = 0$, reduces to Eq. (25) with an equal sign replacing the inequality. Notice that the fourth-order tensors $\mathbf{A}$, $\mathbf{B}$ and $\mathbf{C}$ introduced in Eqs. (13) and (17) can be written as:

$$\mathbf{A} = -\frac{F_{,\phi}}{T}\mathbf{QP} + \mathcal{O}(1),$$

$$\mathbf{B} = -\frac{F_{,\phi}}{T}\mathbf{QP} + \mathcal{O}(1), \tag{26}$$

$$\mathbf{C} = H\left(\frac{F_{,\phi}}{T}\right)^2 \mathbf{QP} + \mathcal{O}(T^{-1}),$$

to the leading order in T, using the definitions for $\mathbf{P}$ and $\mathbf{Q}$ found in Eq. (24).

By inspection, for the asymptotic analysis to proceed, the following expansions should be satisfied by $\Delta\mathbf{u}$, $\Delta\dot{\mathbf{u}}$ and Λ

$$\Delta\mathbf{u} = T\Delta\mathbf{u}_1 + \mathcal{O}(T^2), \quad \Delta\dot{\mathbf{u}} = \Delta\dot{\mathbf{u}}_0 + \mathcal{O}(T), \quad \Lambda = \frac{1}{T}\Lambda_{-1} + \mathcal{O}(1), \tag{27}$$

where $\Delta\mathbf{u}_1$, $\Delta\dot{\mathbf{u}}_0$ and Λ_{-1} are independent of T. Introducing Eqs. (26) and (27) into Eq. (22) and recalling the definitions of the linear operators $\mathscr{E}$, $\mathscr{A}$, $\mathscr{B}$ and $\mathscr{C}$, one obtains

$$\begin{aligned}
&\int_V \delta\mathbf{u}\nabla : \left(\mathbf{L} : \Delta\dot{\mathbf{u}}_0\nabla - F_{,\phi}\mathbf{QP} : \Delta\mathbf{u}_1\nabla\right) \mathrm{d}V = 0, \\
&\int_V \delta\mathbf{u}\nabla : \left[\left(\Lambda_{-1}\mathbf{L} - F_{,\phi}\mathbf{QP}\right) : \Delta\dot{\mathbf{u}}_0\nabla + H\left(F_{,\phi}\right)^2\mathbf{QP} : \Delta\mathbf{u}_1\nabla\right] \mathrm{d}V = 0.
\end{aligned} \tag{28}$$

Inserting the first equation in (28) into the second to eliminate the tensor $\mathbf{L}$ results in

$$\int_V \left(\delta\mathbf{u}\nabla : \mathbf{Q}F_{,\phi}\right)\left\{\mathbf{P} : \left[-\Delta\dot{\mathbf{u}}_0\nabla + \left(\Lambda_{-1} + HF_{,\phi}\right)\Delta\mathbf{u}_1\nabla\right]\right\} \mathrm{d}V = 0. \tag{29}$$

Note that the first term in parenthesis of the integrand in Eq. (29) is a scalar quantity. Consequently, for the integral to vanish for any admissible displacement $\delta\mathbf{u}$, it is necessary that the rest of the integrand be identical to zero, pointwise over the domain of interest. This condition provides the following relation between $\Delta\dot{\mathbf{u}}_0\nabla$ and $\Delta\mathbf{u}_1\nabla$:

$$\mathbf{P} : \Delta\dot{\mathbf{u}}_0\nabla = \left(\Lambda_{-1} + HF_{,\phi}\right)\mathbf{P} : \Delta\mathbf{u}_1\nabla, \tag{30}$$

for all $\mathbf{x} \in V$. Introducing the last result into the first equation in (28), one obtains

$$\int_V \delta\mathbf{u}\nabla : \left(\mathbf{L} - \frac{\mathbf{QP}}{\boldsymbol{\Lambda}_{-1}/F_{,\boldsymbol{\phi}} + H}\right) : \Delta\dot{\mathbf{u}}_0\nabla \, \mathrm{d}V = 0. \tag{31}$$

Comparing the fourth-order tensor entering the linear stability criterion (31) to the incremental moduli tensor in Eq. (25) for the rate-independent case, we

observe that they are identical at neutral stability ($\Lambda_{-1} = 0$). Thus, for the case of an associated flow rule ($\phi = \psi$), positive definiteness of the quadratic form in Eq. (31) associated with $\Lambda_{-1} \leq 0$ implies stability of the stress state in question, since for a symmetric operator $\Lambda = \Lambda^{S}$.

For the case of a non-associated flow rule ($\phi \neq \psi$), $\Lambda_{-1} \geq 0$ is a sufficient condition for the onset of instability, with $\Lambda_{-1} = 0$ marking the onset of either a bifurcation or a limit load. For $\Lambda_{-1} < 0$ (i.e., $\Lambda < 0$), the non-positivity of Λ^{S} cannot be guaranteed and hence no definite conclusion about the solid's linear stability can be drawn. However, it is worth noting that for frictional, cohesive solids, although the operator in Eq. (31) is non self-adjoint, its eigenvalues are real, see discussion in Triantafyllidis and Leroy (1994), and hence the issue of a flutter instability never arises.

4. Application and results

The present section pertains to the application of the proposed linear stability criterion to the plane strain tension and compression of a rectangular block with aspect ratio $r \equiv L_1/L_2$, whose initial configuration is depicted in Fig. 1(a). A finite strain formulation of the problem is adopted and the generalization of the governing equations in Section 2.1 is given in Appendix A. The procedure to solve the corresponding eigenvalue problem (22) is presented in Appendix B. This problem is selected because it has the same geometry used to study the bifurcation of rate-independent solids in either tension (Hill and Hutchinson, 1975) or

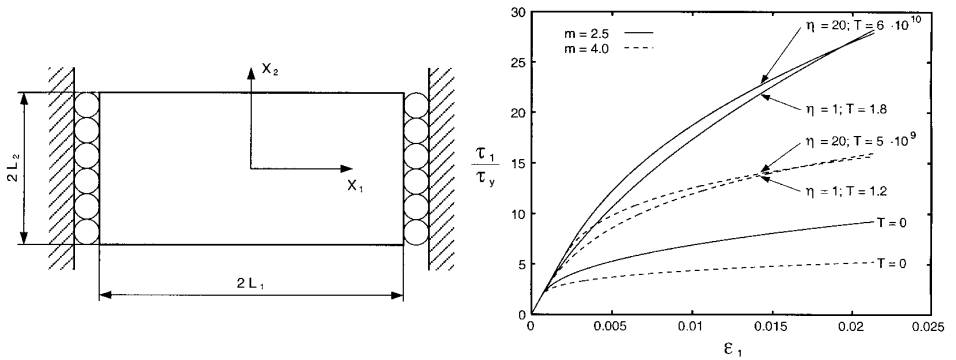

Fig. 1. (a) The plane strain boundary value problem consists of a finitely strained rectangular block of initial dimensions $2L_1 \times 2L_2$, made of an elastic–viscoplastic material. The block is held between two lubricated rigid supports and is subjected either to compressive or to tensile loading along the X_1-direction. (b) The uniaxial stress–strain curves are presented for two values of the hardening exponent m and for the linear overstress ($\eta = 1$) and power-law ($\eta = 20$) viscoplasticity models.

compression (Young, 1976), including non-associated flow rules (Needleman, 1979).

The block is composed of a power-law type rate-dependent solid, which is frequently employed in the studies of elastic–viscoplastic structures, namely

$$\frac{\mathrm{d}\gamma}{\mathrm{d}t} = \Gamma_0 \mathscr{H}\left[\left(\frac{\phi(\boldsymbol{\sigma})}{g(\gamma)}\right)^{\eta} - 1\right], \tag{32}$$

where Γ_0 and η are the reference strain rate and the strain rate exponent, respectively. For metals, typical values of η range from 20 to 50. Furthermore, selecting a value of 1 for η leads to a simple linear overstress model which is similar to the model used in paper 1. The equivalent stress $\phi(\boldsymbol{\sigma})$, as in the time-independent Drucker–Prager yield criterion, equals the sum of the equivalent shear stress based on the J_2 invariant and the mean stress multiplied by the friction coefficient μ. Note that setting μ to zero provides a classical von Mises yield criterion. The hardening function $g(\gamma)$ is found implicitly from

$$\frac{\gamma}{\gamma_{\mathrm{y}}} = \left(\frac{g}{\tau_{\mathrm{y}}}\right)^{m} - m\left(\frac{g}{\tau_{\mathrm{y}}}\right) + m - 1; \quad \gamma \geq 0, \tag{33}$$

where m, τ_{y} and γ_{y} are the hardening exponent, the yield stress in pure shear and the associated shear strain, respectively. The above choice corresponds to a Ramberg–Osgood uniaxial response.

With the introduction of a specific viscosity function in Eq. (32), we are now in a position to compute the characteristic relaxation time t_{R}, which is chosen to be the relaxation time from a steady shear flow stress $2\tau_0$ to τ_0, thus giving

$$t_{\mathrm{R}} = \frac{\tau_0}{\Gamma_0 G}\frac{1}{2^{\eta} - 1}, \tag{34}$$

in which G is the elasticity modulus in shear.

The displacement control loading is chosen so that the dimensionless rate of stretching $\dot{\lambda}_1$ equals 1 or -1 for tension and compression, respectively. This choice is equivalent to setting

$$t_{\mathrm{L}} = \frac{\Delta}{v} = 1, \tag{35}$$

where Δ is the relative displacement of the two ends of the block and v is the corresponding velocity.

The numerical values used in the calculations are: the Poisson's ratio $\nu = 0.3$, the yield strain in pure shear $\gamma_{\mathrm{y}} = 10^{-3}$ and the shear stress τ_0 is set to τ_{y}. The results reported are normalized by $\tau_{\mathrm{y}} = 1$, which gives a shear modulus of $G = 10^3$. The reference strain rate Γ_0 is calculated from the relaxation time t_{R} in Eq. (34), which is deduced from the value of T since t_{L} is set to 1 in Eq. (35).

With this information, the stress–strain curves are presented in Fig. 1(b) in

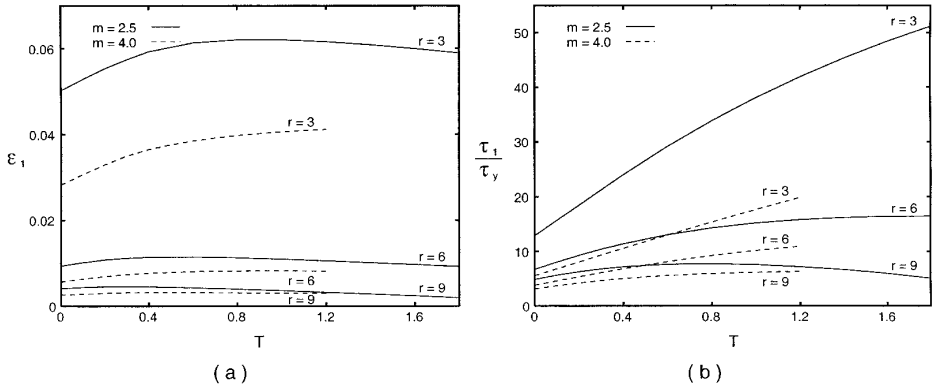

Fig. 2. (a) The critical logarithmic strain and (b) the normalized critical stress in compression are plotted as functions of T and r, for the linear overstress viscosity model ($\eta = 1$). The hardening exponent m is either 2.5 (solid lines) or 4.0 (dashed lines).

which τ_1 is the principal Kirchhoff stress and ϵ_1 is the principal strain, both in direction 1[2]. The two values of the hardening exponent m selected are 2.5 and 4.0. For each value of m, the rate-independent stress–strain curve is shown for $T = 0$. The range of the dimensionless number T studied was selected such that at a strain of 2% the stresses for the two values of the viscosity exponent η of 1 and 20 are approximately three times larger than their rate-independent counterparts. The principal solution for the finite strain tension and compression of the block, based on Eqs. (32)–(35) and Appendix A, is obtained numerically using a fourth-order Runge–Kutta method.

The rest of this section is devoted to the presentation of the stability results, in the form of the critical stress τ_1 and the critical logarithmic strain ϵ_1, evaluated at the stability threshold, defined for a zero eigenvalue Λ in Eq. (22). The corresponding eigenmode in compression is always found to be the long-wavelength antisymmetric S mode. Results for both, the linear overstress model and the power-law viscosity model are presented. For the case of the tensile loading, the corresponding critical eigenmode is always the long-wavelength symmetric necking-type mode. Only the power-law viscosity model is explored in tension. Finally, the friction coefficient set to zero for the earlier calculations is selected to be $\mu = 0.3$, to study the influence of non-associated flow rule on stability. Further information on the stability analysis is given in Appendix B.

The stability results for the compressive loading of the linear overstress model ($\eta = 1$) are presented in Figs. 2 and 3. In Fig. 2(a) and (b), the critical strain and the normalized critical stress are given as functions of the dimensionless number

[2] Recall that for an updated Lagrangian description the Kirchhoff stress tensor $\boldsymbol{\tau}$ is equal to the second Piola-Kirchhoff stress tensor $\mathbf{S}$, required by our general analysis at finite strains.

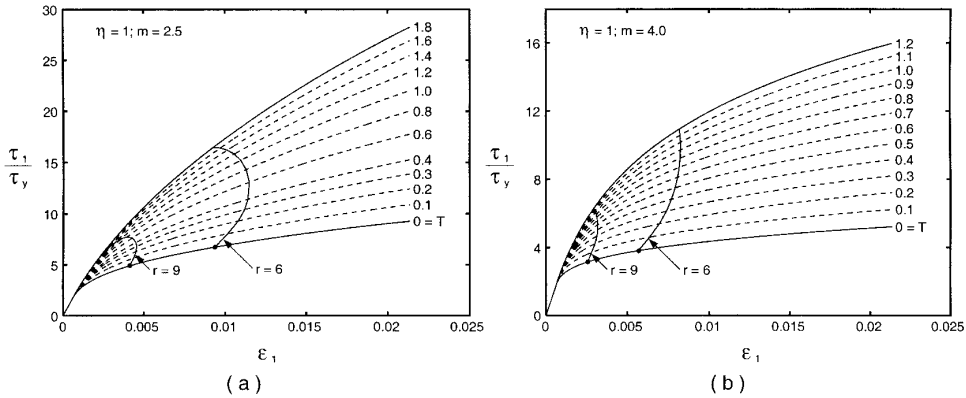

Fig. 3. The critical stresses and strains in compression are superposed to the stress–strain curves obtained for different values of T and r. The hardening exponent m is 2.5 in (a) and 4.0 in (b). The viscosity law is the linear overstress model ($\eta = 1$). The lower solid curve corresponds to the rate-independent problem and the solid dots mark the first failure of Hill's stability criterion.

T. The two values of the hardening exponent considered are $m = 2.5$ depicted by solid lines and $m = 4.0$ depicted by dashed lines. Three values of the block aspect ratio are also studied, the slenderest block corresponding to $r = 9$ and the stubbiest to $r = 3$. In the limit of vanishing T, all the results tend to the critical stress and strain for the first failure of Hill's stability criterion, in accordance with the discussion in Section 3. As expected, the critical stress and strain for the block decrease, as its slenderness increases, i.e., as the ratio r increases. Observe from Fig. 2(a) that for $m = 2.5$, the critical strain is first an increasing function of T, which then passes through a maximum before decreasing. This finding is also clearly seen from Fig. 3(a) in which the stability predictions are superposed to the stress–strain curves obtained for various values of T. We do observe that the curve connecting the loci of all the neutral stability thresholds has the maximum in critical strain, whereas the critical stress keeps increasing with T. Only for the slenderest block ($r = 9$), the critical stress decreases with T after passing through a maximum, which can be seen in Fig. 2(b) for $m = 2.5$. This finding is not completely surprising in view of the results obtained in paper 1 for Shanley's column, which should be indicative here for slender geometry. In paper 1, it was found that the critical load, called the rate-dependent tangent modulus load, was a decreasing function of T. Here, we confirmed that trend only for a certain range of T.

The dependence of the critical stress and strain on T is sensitive to the value of the hardening exponent selected, as can be seen by comparing Fig. 3(a) and (b). For $m = 4.0$, the critical stress is always a monotonically increasing function of T, independent of the aspect ratio. The decrease of the critical strain with T is less pronounced for $m = 4.0$ than for $m = 2.5$. Moreover, the maximal critical strain occurs for larger T if $m = 4.0$.

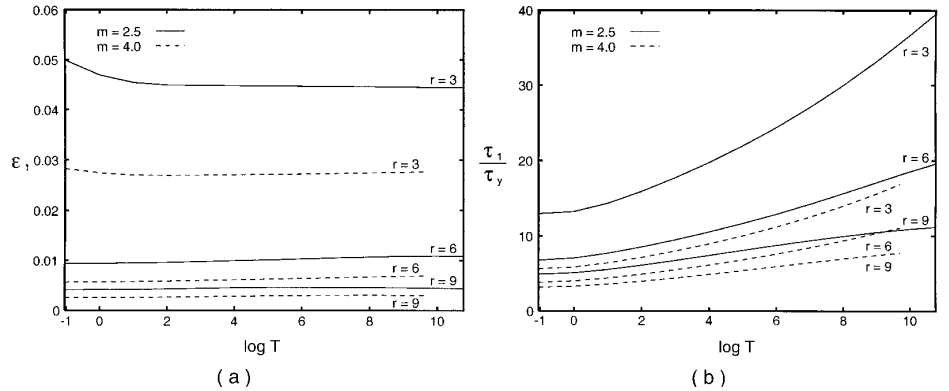

Fig. 4. (a) The critical logarithmic strain and (b) the normalized critical stress in compression are plotted as functions of the logarithm of T and r, for the power-law viscosity model ($\eta = 20$). The hardening exponent m is either 2.5 (solid lines) or 4.0 (dashed lines).

The results for compression with the power-law viscosity model ($\eta = 20$) are presented in the same way in Figs. 4 and 5, except that the dimensionless number T is replaced by its logarithm. The stability predictions are different from the ones obtained with the linear overstress model and are less sensitive to T. The critical strain is found to be an increasing function of T for a slender block ($r = 6, 9$) regardless of the hardening exponent m. On the other hand, it is for a rather stubby specimen ($r = 3$) that the critical strain decreases with T for $m = 2.5$, as can be seen in Fig. 4(a). For $m = 4.0$, the critical strain is also a decreasing function of T until it reaches a minimum at $T \approx 100$. Such a result could not be found in paper 1 since only the linear viscosity function was considered. In

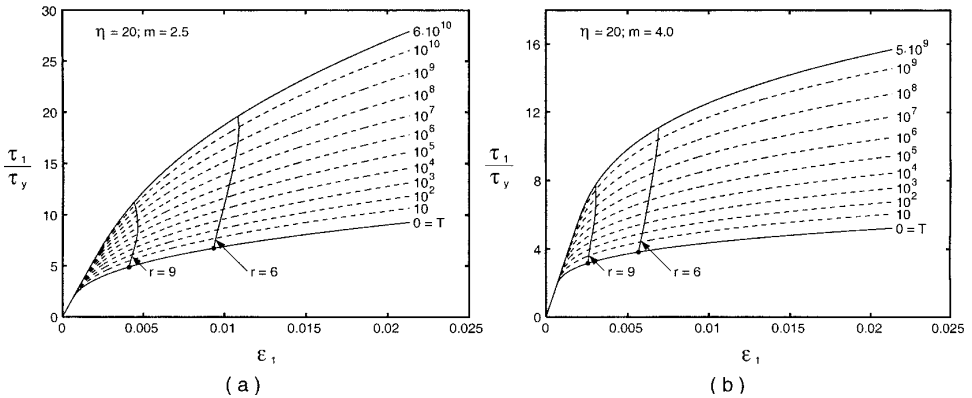

Fig. 5. The critical stresses and strains in compression are superposed to the stress–strain curves obtained for different values of T and r. The hardening exponent m is 2.5 in (a) and 4.0 in (b). The viscosity law is the power-law model ($\eta = 20$). The lower solid curve corresponds to the rate-independent problem and the solid dots mark the first failure of Hill's stability criterion.

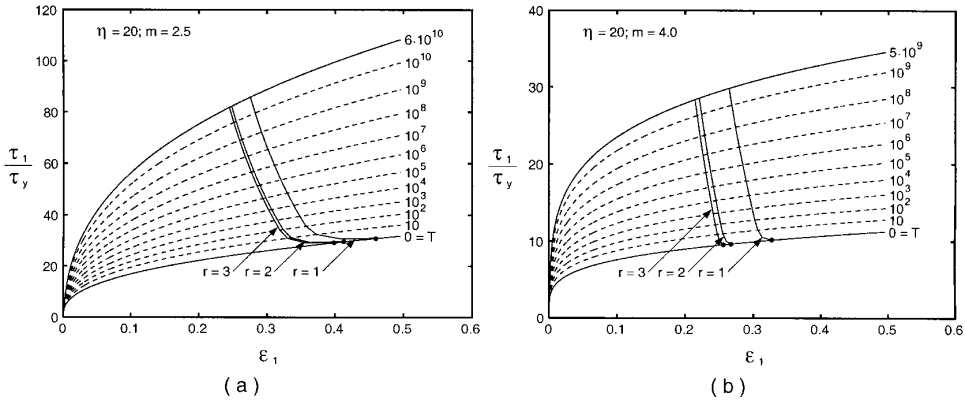

Fig. 6. The critical stresses and strains in tension are superposed to the stress–strain curves obtained for different values of T and r. The hardening exponent m is 2.5 in (a) and 4.0 in (b). The viscosity law is the power-law model ($\eta = 20$). The lower solid curve corresponds to the rate-independent problem and the solid dots mark the first failure of Hill's stability criterion.

contrast to the linear overstress model, the critical stress is always increasing with T, independent of the aspect ratio r or the hardening exponent m.

The stability predictions for the tensile loading of the power-law viscosity model ($\eta = 20$) are presented in Fig. 6 in which the neutral stability predictions are superposed to the stress-strain curves obtained for different values of T. Three aspect ratios are studied, corresponding to $r = 1, 2$ and 3. The critical strain is found to be a decreasing function of T for all values of the aspect ratio r and the hardening exponent m. The critical stress is an increasing function of T except for

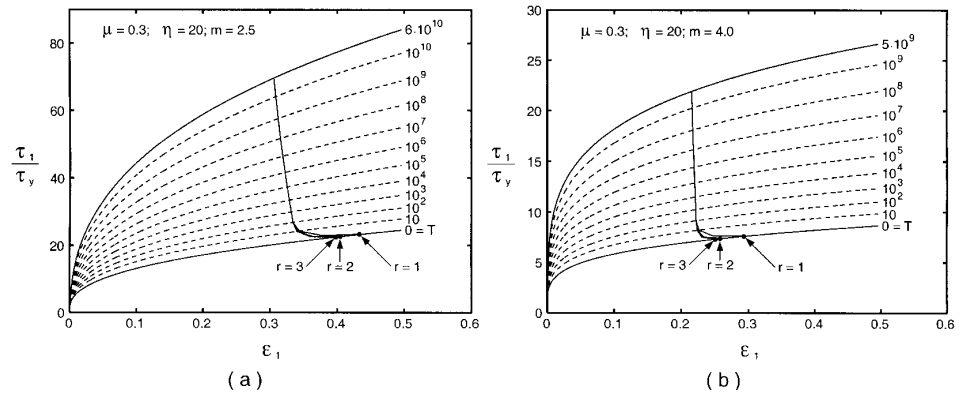

Fig. 7. The critical stresses and strains in tension are superposed to the stress–strain curves obtained for different values of T and r. The hardening exponent m is 2.5 in (a) and 4.0 in (b). The viscosity law is the power-law model ($\eta = 20$). The lower solid curve corresponds to the rate-independent problem and the solid dots mark the first bifurcation of the rate-independent block. The new feature is that the plasticity model has a non-associated flow rule (Drucker–Prager type) with the friction coefficient of $\mu = 0.3$.

$m = 2.5$ and $T < 1$. The influence of r remains small, as it is expected in the presence of the maximum load controlled essentially by the hardening exponent m in the rate-independent limit.

The last point to be discussed is the influence of the friction coefficient μ which was set to zero so far. The results presented in Fig. 7 are for $\mu = 0.3$ and are obtained for the tensile loading of the power-law viscosity model ($\eta = 20$). This case is considered here as an illustration of the capability of the proposed criterion to include non-associated plasticity models. For this class of models, our predictions can be compared to the corresponding self-adjoint case ($\mu = 0$) in Fig. 6. We observe that the critical strain and stress retain the same dependence on the dimensionless number T, but the influence of the aspect ratio vanishes with increasing T for $\mu = 0.3$.

Finally, note that in all the calculations reported above, the stability eigenvalue is always found to be a real number at criticality. By continuity, Λ the dominant eigenvalue of $\mathscr{L}$ in Eq. (19) is also real, which excludes the flutter type instability. Similar results were also obtained by Triantafyllidis and Leroy (1994).

5. Conclusion

The linear stability criterion proposed for rate-sensitive solids and structures provides sufficient conditions for the initially positive growth of a perturbation in the time-dependent solution (trajectory) under investigation. The theory is applicable to a wide range of elastic–viscoplastic solids with non-associated plasticity laws, which undergo finite straining and when inertia effects are negligible. Two relevant characteristic times enter this class of problems: the first associated with the rate of loading and the second with the material viscosity. Their ratio denoted by T plays a predominant role in the stability analysis.

The criterion is based on the initial time evolution of the L_2 norm of the perturbation velocity — a straightforward, but not unique choice for a measure of the perturbation. Due to the technical difficulties in calculating the maximum of the initial time-derivative of this norm, a sufficient condition for linear instability is given which ensures that if the maximum eigenvalue of the operator relating the first and second initial time-derivatives of the perturbation is positive, then the maximum time-derivative of the perturbation norm is also positive and hence the structure is initially unstable.

There are at least two limitations to the proposed method. First, the size of the perturbation has to be small enough to maintain the loading conditions of the trajectory. Second, only the initial stability of the trajectory is assessed this way. The study of stability over a finite time interval requires a full solution of the perturbation problem, frequently possible only by numerical means.

There are however advantages of the proposed method. To start with, the initial development of the perturbation is calculated exactly, without any of the assumptions required by the frozen coefficients method. Moreover, the methodology is applicable to a general class of materials including non-associated

flow rules. Also, for the dimensionless number T approaching zero and for the case of associated flow rule, the method reduces to the study of Hill's stability functional for rate-independent solids, for which the loss of positive definiteness signals the onset of instability.

The method was applied to the stability of a finitely strained rectangular block under plane strain tension and compression, starting from a stress-free configuration. It is of interest that the critical strains and stresses corresponding to the first instability are not monotonic functions of the dimensionless number T. In the limit of $T \to 0$, the critical stress found coincides with the first bifurcation point of the equilibrium path.

As previously mentioned, a fundamental assumption in our linear stability analysis of rate-dependent solids is that, the loading conditions of the principal trajectory remain unchanged by the perturbation. This assumption precludes the consideration of arbitrary perturbations and also the study of equilibrium stability, which is the subject of future research.

Acknowledgements

M.N. and N.T. would like to acknowledge the partial support by AFOSR Grant: F49620-99-1-0098 to the University of Michigan. Y.L., currently Visiting Professor of Aerospace Engineering, would like to thank the Aerospace Department and the College of Engineering for their hospitality and support.

Appendix A. Extension to finite strains

The extension of the proposed linear stability criterion to account for finite strains is now outlined using a full Lagrangian formulation and a fixed Cartesian coordinate system. In the reference configuration, a rate-dependent solid occupies the volume V bounded by the surface ∂V. The equations of equilibrium, expressed by the principle of virtual work (no body force), are[3]

$$\int_V S_{ij}\delta E_{ij}\,\mathrm{d}V = \int_{\partial V} T_i \delta u_i\,\mathrm{d}S, \tag{A1}$$

where $\mathbf{S}$, $\mathbf{T}$, $\mathbf{E}$ and $\mathbf{u}$ are the second Piola–Kirchhoff stress tensor, the traction on part of the surface ∂V, the Lagrangian strain tensor and the displacement field, respectively.

For finitely strained solids, a convenient form of the constitutive law is given, in the current configuration, by the elasticity tensor $\mathbf{L}^{\mathrm{e}}$ which relates the Jaumann rate of the Kirchhoff stress to the elastic part of the strain rate tensor. In the

[3] Here and subsequently, Einstein's summation convention is implied over repeated indexes. Repeated indexes in parentheses are not summed, unless indicated explicitly.

reference configuration, this constitutive law is given by

$$\dot{S}_{ij} = L^{\mathrm{e}}_{ijkl}\left(\dot{E}_{kl} - \dot{E}^{\mathrm{p}}_{kl}\right) + G_{ijkl}\dot{E}_{kl}, \tag{A2}$$

in which the elasticity tensor $\mathbf{L}^{\mathrm{e}}$ and the geometric tensor $\mathbf{G}$ have the standard definitions in continuum mechanics (see for example Eqs. (20) and (21) in Triantafyllidis and Leroy, 1994). In addition, $\dot{\mathbf{E}}^{\mathrm{p}}$ is the plastic part of the Lagrangian strain rate tensor $\dot{\mathbf{E}}$ and is given by the following flow rule:

$$\dot{E}^{\mathrm{p}}_{ij} = \dot{\gamma}\frac{\partial \psi}{\partial S_{ij}}, \tag{A3}$$

where the flow potential $\psi(\mathbf{S})$ is now a function of the second Piola–Kirchhoff stress tensor. The equivalent plastic strain rate $\dot{\gamma}$ is governed by Eq. (5), in which the equivalent stress $\phi(\mathbf{S})$ is now also defined in terms of the second Piola–Kirchhoff stress tensor. The flow potential ψ and the equivalent stress ϕ are expressed in terms of the equivalent shear stress $Q(\mathbf{S})$ and the equivalent pressure $P(\mathbf{S})$ by

$$\begin{gathered}\psi = Q(\mathbf{S}) + \beta P(\mathbf{S}) \quad \text{and} \quad \phi = Q(\mathbf{S}) + \mu P(\mathbf{S}), \\ \text{where } Q \equiv \left(\frac{1}{2}S'_{ij}C_{ik}C_{jl}S'_{kl}\right)^{1/2} \text{ and } P \equiv \frac{1}{3}S_{ij}C_{ij};\ S'_{ij} \equiv S_{ij} - PC^{-1}_{ij},\end{gathered} \tag{A4}$$

in which $\mathbf{S}'$ is the deviatoric second Piola–Kirchhoff stress tensor and $\mathbf{C}$ is the right Cauchy–Green tensor. Also, β and μ are the dilatancy parameter and the friction coefficient of the material, respectively. Note that in all the calculations presented in Section 4, the dilatancy parameter β is set to zero.

Following the general methodology presented in Section 2, by linearizing the first and second time-derivatives of the principle of virtual work (A1) and accounting for (A2)–(A4), we obtain the equations governing the initial evolution of the perturbation

$$\begin{gathered}\int_V \delta u_{i,\,j}\left(L_{ijkl}\Delta\dot{u}_{k,\,l} + A_{ijkl}\Delta u_{k,\,l}\right)\mathrm{d}V = 0, \\ \int_V \delta u_{i,\,j}\left[\left(\Lambda L_{ijkl} + B_{ijkl}\right)\Delta\dot{u}_{k,\,l} + C_{ijkl}\Delta u_{k,\,l}\right]\mathrm{d}V = 0.\end{gathered} \tag{A5}$$

Finally, to the leading order term in T the tensors $\mathbf{A}$, $\mathbf{B}$ and $\mathbf{C}$ are

$$A_{ijkl} = -\frac{F_{,\phi}}{T}L^{\mathrm{e}}_{ijmn}\frac{\partial \psi}{\partial S_{mn}}\left[\frac{\partial \phi}{\partial E_{kl}} + \frac{\partial \phi}{\partial S_{pq}}\left(L^{\mathrm{e}}_{pqkl} + G_{pqkl}\right)\right] + \mathcal{O}(1),$$

$$B_{ijkl} = -\frac{F_{,\phi}}{T} L^{\mathrm{e}}_{ijmn} \frac{\partial \psi}{\partial S_{mn}} \left[\frac{\partial \phi}{\partial E_{kl}} + \frac{\partial \phi}{\partial S_{pq}} \left(L^{\mathrm{e}}_{pqkl} + G_{pqkl} \right) \right] + \mathcal{O}(1), \tag{A6}$$

$$C_{ijkl} = H \left(\frac{F_{,\phi}}{T} \right)^2 L^{\mathrm{e}}_{ijmn} \frac{\partial \psi}{\partial S_{mn}} \left[\frac{\partial \phi}{\partial E_{kl}} + \frac{\partial \phi}{\partial S_{pq}} \left(L^{\mathrm{e}}_{pqkl} + G_{pqkl} \right) \right] + \mathcal{O}(T^{-1}),$$

where H is identical to the one appearing in Eq. (24), except for the Cauchy stress tensor now being the second Piola–Kirchhoff stress tensor.

Two remarks are now in order. First, it was impossible to present concisely, the complete expressions for the finite strain version of the tensors **A**, **B** and **C**, and the interested reader is referred to Nestorović (2001). Second, the leading order term in T of these tensors is necessary for obtaining the finite strain version of the fourth-order tensor entering the linear stability criterion (31), in the limit of vanishing T. Notice from Eq. (A6) that the first term in brackets ($\partial\phi/\partial \boldsymbol{E}$) and the geometric term **G** would not be present, if the tensors were constructed by direct generalization of the small strain counterparts to finite strain. This slight difference renders impossible an exact comparison of our bifurcation results and the ones found in the classical analyses of rate-independent solids, evoked at the beginning of Section 4.

Appendix B. Formulation and solution procedure for a rectangular block

The eigenvalue problem and the solution procedure for the stability of a rate-dependent rectangular block are provided here. The rectangular block has length $2L_1$ and width $2L_2$ in its undeformed stress-free configuration, depicted in Fig. 1(a). The block is deformed uniformly so that in the current configuration the material occupies the region V defined by $-l_i \leq x_i \leq +l_i$, where x_i are the current coordinates of a material point relative to a fixed Cartesian coordinate system and $l_i = \lambda_i L_i$ with λ_i the stretch ratios of the block. The two ends $x_1 = \pm l_1$ are assumed to remain flat and free of shear.

The initial absence of the shear stresses coupled with the initial isotropy of the material produces principal stresses aligned with the two axes and results in material orthotropy, which in turn implies that the "normal-to-shear" components of the tensors **L**, **A**, **B** and **C** are equal to zero. With this simplification, the governing (Euler–Lagrange) equations in V, obtained from $(\mathrm{A5})_1$ reduce to

$$\begin{aligned} &L_{1111}\Delta\dot{u}_{1,\,11} + L_{1122}\Delta\dot{u}_{2,\,21} + L_{1212}\Delta\dot{u}_{1,\,22} + L_{1221}\Delta\dot{u}_{2,\,12} \\ &\quad + A_{1111}\Delta u_{1,\,11} + A_{1122}\Delta u_{2,\,21} + A_{1212}\Delta u_{1,\,22} + A_{1221}\Delta u_{2,\,12} = 0, \\ &L_{2121}\Delta\dot{u}_{2,\,11} + L_{2112}\Delta\dot{u}_{1,\,21} + L_{2211}\Delta\dot{u}_{1,\,12} + L_{2222}\Delta\dot{u}_{2,\,22} \\ &\quad + A_{2121}\Delta u_{2,\,11} + A_{2112}\Delta u_{1,\,21} + A_{2211}\Delta u_{1,\,12} + A_{2222}\Delta u_{2,\,22} = 0, \end{aligned} \tag{B1}$$

while from $(\mathrm{A5})_2$ become

$$(\Lambda L_{1111} + B_{1111})\Delta\dot{u}_{1,\,11} + (\Lambda L_{1122} + B_{1122})\Delta\dot{u}_{2,\,21} + (\Lambda L_{1212} + B_{1212})\Delta\dot{u}_{1,\,22}$$
$$+ (\Lambda L_{1221} + B_{1221})\Delta\dot{u}_{2,\,12} + C_{1111}\Delta u_{1,\,11} + C_{1122}\Delta u_{2,\,21} + C_{1212}\Delta u_{1,\,22}$$
$$+ C_{1221}\Delta u_{2,\,12} = 0, \tag{B2}$$

$$(\Lambda L_{2121} + B_{2121})\Delta\dot{u}_{2,\,11} + (\Lambda L_{2112} + B_{2112})\Delta\dot{u}_{1,\,21} + (\Lambda L_{2211} + B_{2211})\Delta\dot{u}_{1,\,12}$$
$$+ (\Lambda L_{2222} + B_{2222})\Delta\dot{u}_{2,\,22} + C_{2121}\Delta u_{2,\,11} + C_{2112}\Delta u_{1,\,21} + C_{2211}\Delta u_{1,\,12}$$
$$+ C_{2222}\Delta u_{2,\,22} = 0.$$

The requirement that the two ends $x_1 = \pm l_1$ remain flat implies that there is no perturbation in displacement normal to the two edges. The boundary conditions resulting from Eq. (A5), on the two edges $x_1 = \pm l_1$ are:

$$\Delta u_{1,\,2} = \Delta\dot{u}_{1,\,2} = 0 \quad \text{and} \quad \Delta\dot{u}_{2,\,1} = \Delta u_{2,\,1} = 0, \tag{B3}$$

while on the other two traction-free edges $x_2 = \pm l_2$ are:

$$L_{1212}\Delta\dot{u}_{1,\,2} + L_{1221}\Delta\dot{u}_{2,\,1} + A_{1212}\Delta u_{1,\,2} + A_{1221}\Delta u_{2,\,1} = 0,$$

$$L_{2211}\Delta\dot{u}_{1,\,1} + L_{2222}\Delta\dot{u}_{2,\,2} + A_{2211}\Delta u_{1,\,1} + A_{2222}\Delta u_{2,\,2} = 0, \tag{B4}$$

$$(\Lambda L_{1212} + B_{1212})\Delta\dot{u}_{1,\,2} + (\Lambda L_{1221} + B_{1221})\Delta\dot{u}_{2,\,1} + C_{1212}\Delta u_{1,\,2} + C_{1221}\Delta u_{2,\,1} = 0,$$

$$(\Lambda L_{2211} + B_{2211})\Delta\dot{u}_{1,1} + (\Lambda L_{2222} + B_{2222})\Delta\dot{u}_{2,2} + C_{2211}\Delta u_{1,1} + C_{2222}\Delta u_{2,\,2} = 0.$$

The independent variables x_i can be decoupled for the modes Δu_i and $\Delta\dot{u}_i$, and the governing Eqs. (B1) and (B2) are satisfied by solutions in the form

$$\begin{bmatrix} \Delta\dot{u}_1 \\ \Delta u_1 \end{bmatrix} = \begin{bmatrix} -V_1(x_2) \\ -U_1(x_2) \end{bmatrix} \sin p_1 x_1, \quad \begin{bmatrix} \Delta\dot{u}_2 \\ \Delta u_2 \end{bmatrix} = \begin{bmatrix} V_2(x_2) \\ U_2(x_2) \end{bmatrix} \cos p_1 x_1,$$
$$\text{with} \quad p_1 = \frac{n\pi}{l_1}, \tag{B5}$$

and also in the form

$$\begin{bmatrix} \Delta\dot{u}_1 \\ \Delta u_1 \end{bmatrix} = \begin{bmatrix} V_1(x_2) \\ U_1(x_2) \end{bmatrix} \cos p_1 x_1, \quad \begin{bmatrix} \Delta\dot{u}_2 \\ \Delta u_2 \end{bmatrix} = \begin{bmatrix} V_2(x_2) \\ U_2(x_2) \end{bmatrix} \sin p_1 x_1,$$
$$\text{with} \quad p_1 = \frac{(n - \frac{1}{2})\pi}{l_1}, \tag{B6}$$

where $V_i(x_2)$ and $U_i(x_2)$ $(i = 1, 2)$ are at least twice-differentiable functions in x_2 and $n = 1, 2, \ldots$ are the positive integers. Note that the solution of the form (B5) is symmetric in x_1, while (B6) is antisymmetric in x_1. Also, note that these two

choices for modes identically satisfy the boundary conditions (B3) on the two ends $x_1 = \pm l_1$. The functions $V_i(x_2)$ and $U_i(x_2)$ introduced in Eqs. (B5) and (B6) are of the form

$$
\begin{aligned}
V_1(x_2) &= \sum_{m=1}^{4}\Big[V_1^{(m)}\big(\xi_{(m)}\mathscr{S}_{(m)} + \eta_{(m)}\mathscr{A}_{(m)}\big)\Big],\\
V_2(x_2) &= \sum_{m=1}^{4}\Big[V_2^{(m)}\big(\xi_{(m)}\mathscr{A}_{(m)} + \eta_{(m)}\mathscr{S}_{(m)}\big)\Big],\\
U_1(x_2) &= \sum_{m=1}^{4}\Big[U_1^{(m)}\big(\xi_{(m)}\mathscr{S}_{(m)} + \eta_{(m)}\mathscr{A}_{(m)}\big)\Big],\\
U_2(x_2) &= \sum_{m=1}^{4}\Big[U_2^{(m)}\big(\xi_{(m)}\mathscr{A}_{(m)} + \eta_{(m)}\mathscr{S}_{(m)}\big)\Big],
\end{aligned}
\tag{B7}
$$

with

$$
\begin{aligned}
\mathscr{S}_{(m)}(x_2) &= \exp[\rho_{(m)}p_1x_2] - \exp[-\rho_{(m)}p_1x_2],\\
\mathscr{A}_{(m)}(x_2) &= \exp[\rho_{(m)}p_1x_2] + \exp[-\rho_{(m)}p_1x_2],
\end{aligned}
\tag{B8}
$$

where the following notations have been employed: The functions $\mathscr{S}_{(m)}(x_2)$ and $\mathscr{A}_{(m)}(x_2)$ are the symmetric and antisymmetric mode in x_2, respectively, while $\xi_{(m)}$ and $\eta_{(m)}$ are the amplitudes of the mth partial solution. To ensure that the solution of the form (B5) or (B6) satisfies the governing equations (B1) and (B2), the scalars $\rho_{(m)}$ are defined as the four positive square roots of the fourth-order polynomial in ρ^2 of the following 4×4 matrix:

$$
\det\begin{bmatrix} \mathscr{L}(\rho) & \mathscr{A}(\rho) \\ \Lambda\mathscr{L}(\rho) + \mathscr{B}(\rho) & \mathscr{C}(\rho) \end{bmatrix} = 0. \tag{B9}
$$

The above introduced 2×2 matrices $\mathscr{L}$, $\mathscr{A}$, $\mathscr{B}$ and $\mathscr{C}$ are symbolically represented by

$$
\boldsymbol{\chi}(\rho) = \begin{bmatrix} \rho^2X_{1212} - X_{1111} & \rho(X_{1122} + X_{1221}) \\ -\rho(X_{2112} + X_{2211}) & \rho^2X_{2222} - X_{2121} \end{bmatrix}, \tag{B10}
$$

where X_{ijkl} stands for the corresponding component of the tensors **L**, **A**, **B** or **C**. The unit vector $(\mathbf{V}^{(m)}, \mathbf{U}^{(m)})$, which is associated with $\rho_{(m)}$, is the normalized eigenvector of the following 4×4 matrix:

$$\begin{bmatrix} \mathscr{L}(\rho_{(m)}) & \mathscr{A}(\rho_{(m)}) \\ \Lambda\mathscr{L}(\rho_{(m)}) + \mathscr{B}(\rho_{(m)}) & \mathscr{C}(\rho_{(m)}) \end{bmatrix} \begin{bmatrix} \mathbf{V}^{(m)} \\ \mathbf{U}^{(m)} \end{bmatrix} = 0. \tag{B11}$$

Finally, by substituting the solution of the form (B5) or (B6) into the remaining boundary conditions (B4) on the traction-free edges $x_2 = \pm l_2$, we obtain two decoupled homogeneous systems for $\xi_{(m)}$ and $\eta_{(m)}$

$$\sum_{m=1}^{4} S^{I}_{nm}\xi_{(m)} = 0 \quad \text{and} \quad \sum_{m=1}^{4} S^{II}_{nm}\eta_{(m)} = 0, \tag{B12}$$

in which the components of the 4×4 matrices $\mathbf{S}^{\alpha}$ ($\alpha = I, II$) are given by

$$\begin{aligned}
S^{I}_{1m} &= \left(L_{1212}V^{(m)}_{1}\rho_{(m)} + L_{1221}V^{(m)}_{2} + A_{1212}U^{(m)}_{1}\rho_{(m)} + A_{1221}U^{(m)}_{2}\right)\mathscr{A}_{(m)}(l_2), \\
S^{I}_{2m} &= \left(L_{2211}V^{(m)}_{1} - L_{2222}V^{(m)}_{2}\rho_{(m)} + A_{2211}U^{(m)}_{1} - A_{2222}U^{(m)}_{2}\rho_{(m)}\right)\mathscr{S}_{(m)}(l_2), \\
S^{I}_{3m} &= \Big[(\Lambda L_{1212} + B_{1212})V^{(m)}_{1}\rho_{(m)} + (\Lambda L_{1221} + B_{1221})V^{(m)}_{2} + C_{1212}U^{(m)}_{1}\rho_{(m)} \\
&\quad + C_{1221}U^{(m)}_{2}\Big]\mathscr{A}_{(m)}(l_2), \\
S^{I}_{4m} &= \Big[(\Lambda L_{2211} + B_{2211})V^{(m)}_{1} - (\Lambda L_{2222} + B_{2222})V^{(m)}_{2}\rho_{(m)} + C_{2211}U^{(m)}_{1} \\
&\quad - C_{2222}U^{(m)}_{2}\rho_{(m)}\Big]\mathscr{S}_{(m)}(l_2), \\
S^{II}_{1m} &= \left(L_{1212}V^{(m)}_{1}\rho_{(m)} + L_{1221}V^{(m)}_{2} + A_{1212}U^{(m)}_{1}\rho_{(m)} + A_{1221}U^{(m)}_{2}\right)\mathscr{S}_{(m)}(l_2), \\
S^{II}_{2m} &= \left(L_{2211}V^{(m)}_{1} - L_{2222}V^{(m)}_{2}\rho_{(m)} + A_{2211}U^{(m)}_{1} - A_{2222}U^{(m)}_{2}\rho_{(m)}\right)\mathscr{A}_{(m)}(l_2), \\
S^{II}_{3m} &= \Big[(\Lambda L_{1212} + B_{1212})V^{(m)}_{1}\rho_{(m)} + (\Lambda L_{1221} + B_{1221})V^{(m)}_{2} + C_{1212}U^{(m)}_{1}\rho_{(m)} \\
&\quad + C_{1221}U^{(m)}_{2}\Big]\mathscr{S}_{(m)}(l_2), \\
S^{II}_{4m} &= \Big[(\Lambda L_{2211} + B_{2211})V^{(m)}_{1} - (\Lambda L_{2222} + B_{2222})V^{(m)}_{2}\rho_{(m)} + C_{2211}U^{(m)}_{1} \\
&\quad - C_{2222}U^{(m)}_{2}\rho_{(m)}\Big]\mathscr{A}_{(m)}(l_2).
\end{aligned} \tag{B13}$$

The two homogeneous systems in Eq. (B12) are studied independently and have a non-trivial solution $\xi_{(m)}$ or $\eta_{(m)}$, respectively, when the corresponding matrix of constants is singular. Thus, the loss of stability will correspond to the first such occurrence of a singular matrix $\mathbf{S}^{\alpha}$ $(\alpha = I, II)$ in either of the systems, (at the critical strain ϵ_1^{c} for fixed values of the following: eigenvalue Λ, characteristic number T and product $p_1 l_2$), as the principal strain ϵ_1 increases from zero, i.e.,

$$\det\left[\mathbf{S}^{\alpha}\left(\Lambda, p_1 l_2, T, \epsilon_1^{c}\right)\right] = 0,$$
$$\det\left[\mathbf{S}^{\alpha}(\Lambda, p_1 l_2, T, \epsilon_1)\right] \neq 0 \quad \text{for } 0 \leq \epsilon_1 < \epsilon_1^{c}. \tag{B14}$$

Note that the first occurrence of a singular matrix $\mathbf{S}^{\alpha}$ always corresponds to the positive integer $n = 1$, in Eqs. (B5) and (B6), thus justifying the statement from Section 4 that the critical eigenmode is always of the long-wavelength.

References

Anand, L., Kim, H.K., Shawki, T.G., 1987. Onset of shear localization in viscoplastic solids. J. Mech. Phys. Solids 35, 407–429.

Clifton, R.J., 1978. Adiabatic shear band, in Report NMAB-356 of the US NRC Committee on material response to ultrasonic loading rates.

Hill, R., 1958. A general theory of uniqueness and stability in elastic/plastic solids. J. Mech. Phys. Solids 4, 247–255.

Hill, R., Hutchinson, J.W., 1975. Bifurcation phenomena in the plane tension test. J. Mech. Phys. Solids 23, 239–264.

Hutchinson, J.W., 1974. Plastic buckling. Adv. Appl. Mechanics 14, 67–144.

Leroy, Y.M., 1991. Linear stability analysis of rate-dependent discrete systems. Int. J. Solids Structures 27, 783–808.

Massin, P., Triantafyllidis, N., Leroy, Y.M., 1999. On the stability of strain-rate dependent solids. Part I: Structural examples. J. Mech. Phys. Solids 47, 1737–1779.

Molinari, A., 1997. Collective behavior and spacing of adiabatic shear bands. J. Mech. Phys. Solids 45, 1551–1575.

Needleman, A., 1979. Non-normality and bifurcation in plane strain tension and compression. J. Mech. Phys. Solids 27, 231–254.

Nestorović M.D., 2001. Ph.D. thesis, The University of Michigan, Ann Arbor, USA.

Nguyen, Q.S., Radenkovic, D., 1975. Stability of equilibrium in elastic/plastic solids. In: I.U.T.A.M. Symposium, Marseilles, 403–414.

Shanley, F.R., 1947. Inelastic column theory. J. Aeronaut. Sciences 14, 261–267.

Triantafyllidis, N., Leroy, Y.M., 1994. Stability of a frictional material layer resting on a viscous half-space. J. Mech. Phys. Solids 42, 51–110.

Tvergaard, V., 1985. Rate-sensitivity in elastic–plastic panel buckling, Aspects of the Analysis of Plate Structures, W.A. Wittrick volume, 293–308.

Young, N.J.B., 1976. Bifurcation phenomena in the plane compression test. J. Mech. Phys. Solids 24, 77–91.